Projected fermion ground-state ansatz for the S=1/2 Kagome lattice antiferromagnet

1991 J. Phys.: Condens. Matter 3 8067

(http://iopscience.iop.org/0953-8984/3/41/006)

J. Phys.: Condens. Matter 3 (1991) 8067–8078. Printed in the UK

Projected fermion ground-state *ansatz* for the $S = 1/2$ Kagomé lattice antiferromagnet

T C Hsu† and A J Schofield‡

† Physics Department, University of British Columbia, 6224 Agriculture Road, Vancouver, BC, Canada V6T 2A6

‡ IRC in Superconductivity, University of Cambridge, Madingley Road, Cambridge CB3 0HE, UK

Received 20 May 1991

Abstract. We test the quality of mean field ground states for the $S = 1/2$ Heisenberg antiferromagnet on a Kagomé lattice. These states, motivated by the large-n saddle points of Marston and Zeng, are constructed from eigenstates of single particles hopping on lattices with uniform, staggered or no magnetic fields and their BCS analogues. Short-range spin–spin correlations (up to third-nearest-neighbour) are calculated. They are compared to those obtained by Zeng and Elser from small cluster diagonalization. In all trial states certain second- and third-neighbour correlations are qualitatively distinct from the ground state. The trial state which most resembles the ground state is the projected BCS state. Deviations of second- and third-neighbour correlations from those of the actual ground state do not appear to be due to a lack of spin–Peierls order. We argue that more short-range three-sublattice Néel order should be present. Numerical results suggest a specific choice of sublattice arrangement. We also propose specific changes in two-spin correlations which would be signatures of a transition from a state of one type to another. These may be relevant for the 2.5 mK specific heat peak recently observed in helium-3 films by Greywall and Busch.

1. Introduction

The $S = 1/2$ Heisenberg antiferromagnet (AFM) on a frustrated lattice is a candidate for a two-dimensional system with a quantum spin liquid ground state. The Kagomé lattice AFM is a simple example of such a system. Its classical (three-sublattice Néel ordered) ground state has a continuous, local degeneracy. This is because there exist clusters of sites which are in only two out of the three sublattices and which are surrounded by sites in the remaining sublattice. The sublattice magnetizations inside the cluster can then be rotated about the axis of magnetization of the third sublattice without changing the classical spin energy.

The experimental evidence that this system might be realized in nature comes from heat capacity measurements of Greywall and Busch [1] on thin films of ^{3}He. At coverages corresponding to a partially occupied second layer of atoms, the heat capacity ceases to show Fermi liquid behaviour and has a peak at around 2.5 mK. These experiments have been interpreted by Elser [2] as being due to the second layer forming a registered triangular solid with an anisotropic antiferromagnetic nuclear exchange interaction modelled by a Kagomé lattice. Further experimental insight comes from measurements on Sr–Cr–Ga–O where the $S = 3/2$ Cr^{3+} ions are coordinated

0953-8984/91/418067+12$03.50

in a Kagomé lattice. These materials show a heat capacity [3] proportional to T^2 indicating a gapless, perhaps Goldstone, mode of excitation. On the other hand low-temperature elastic neutron scattering near momenta associated with three-sublattice Néel order shows only a broad maximum corresponding to a correlation length of a few lattice spacings [4,5]. In this paper we study only the $S = 1/2$ system. Our results may shed some light on the $S = 3/2$ system.

Exact diagonalization of the $S = 1/2$ system on small clusters of up to 21 sites has been performed by Zeng and Elser [6]. The system size was too small to identify the form of long-range order in the ground state. Nevertheless, various short-range correlation functions for the ground state up to about third-nearest-neighbour are now available. By a Monte Carlo simulation they obtain a double peak in the heat capacity. Experimentally there is only one peak but only about half the entropy of $\ln 2$ per spin is underneath the peak so there is probably another peak at lower temperature [6]. Thus there may be two ordered states which exist for the Kagomé AFM. Zeng and Elser have also calculated the zero-point correction to the classical three-sublattice Néel ground state by spin waves and found that long-range Néel order does not survive. Consistent with this result are the results of Chandra *et al* [8] who have proposed a novel ground state with long-range order called the spin nematic. This state has a gapless Goldstone mode which explains the low-temperature specific heat in the $S = 3/2$ system but the long-range order would not show up in neutron scattering.

In this paper we concentrate on short-range correlation functions. Our motivation comes from the results of a large-n study of the Kagomé AFM. Marston and Zeng [7] have considered a SU(n) model on the Kagomé lattice. They find that the dimer solid ground state is stable at large n. Such a ground state would probably have a gapped excitation spectrum (incompatible with the spin nematic proposal). But introducing a bi-quadratic coupling, which does not alter the model in the $n = 2$ limit, makes the system unstable to a chiral spin liquid or 'flux' phase above a critical temperature. Other phases which do not break time reversal invariance ('staggered flux' or 'no flux' as defined below) were found to be higher in energy. Sachdev and Read [9] have considered Sp(n) models which are useful in the case of frustrated or doped AFMs. Under this scheme BCS-like paired ground states can result. These are related to similar states considered in the case of the square lattice [10–12].

The purpose of this paper is not to improve on exact diagonalization results, which are limited to small clusters, but to check whether the mean field states considered by Marston and Zeng and BCS-like states are viable ground states for the infinite system. This we do by considering spin wavefunctions based on large-n states and calculating whether they reproduce the known short-range correlation functions. It is known that the relative energies of a valence bond solid or various spin liquid states in the large-n theory may be different from those when $n = 2$ and the constraint is treated exactly. Thus it is necessary to construct explicit wavefunctions for the $S = 1/2$ AFM motivated by large-n saddle points and to compare their spin–spin correlations including the energy. As we shall see, many states can be clearly ruled out as ground-state candidates and so we do not have to worry about sensitive energy minimization upon which the choice of long-range order in the ground state depends.

2. The fermion projection technique

The antiferromagnetic spin correlations of a translationally invariant projected elec-

tron wavefunction are dominated by the nearest-neighbour exchange holes of like-spin electrons [13] or the nearest-neighbour BCS pairing of opposite-spin electrons. The kinetic energy of a single species of fermions is intimately linked to the size of the nearest-neighbour exchange hole and so we may identify good fermion wavefunctions by their total kinetic energy. Similarly the BCS pairing condensation energy is related to the contribution of singlet pairs to the antiferromagnetic spin correlations. The energy of the spin system, being a measure of the nearest-neighbour spin correlations only, is a poor indication of the variational quality of a wavefunction especially when there are low-lying excitations. Therefore, to evaluate the quality of our trial ground states, we compare the first-, second- and third-neighbour spin correlations of our wavefunctions with the results of diagonalization on small clusters.

In this paper we shall be interested in calculating the ground-state expectation $\langle S_i^z S_j^z \rangle$. For a projected fermion state, this expectation value can be written:

$$\langle S_i^z S_j^z \rangle = \sum_{\alpha,\beta} m_{\alpha\beta} \frac{\langle \psi \mid \hat{P}_{d=0}\, c_{i,\alpha}^{\dagger}\, c_{j,\beta}^{\dagger}\, c_{j,\beta}\, c_{i,\alpha}\, \hat{P}_{d=0} \mid \psi \rangle}{\langle \psi \mid \hat{P}_{d=0} \mid \psi \rangle} \tag{1}$$

where $\alpha, \beta = \pm 1$ are spin indices, $m_{\alpha\beta} = \alpha\beta/4$ and

$$\hat{P}_{d=0} = \prod_i (1 - c_{i\uparrow}^{\dagger} c_{i\uparrow} c_{i\downarrow}^{\dagger} c_{i\downarrow})$$

is a projection operator which removes double occupancy. To perform numerical calculations on a projected state, we divide the projection operator into two pieces:

$$\hat{P}_{d=0} = \prod_{x \in A} (1 - n_{x\uparrow} n_{x\downarrow}) \prod_{y \in B} (1 - n_{y\uparrow} n_{y\downarrow})$$

where A and B are a partition of the lattice. B is a cluster that contains the sites i and j in question and A contains all other sites. The projection on set A and its influence on set B may be approximated crudely by a fugacity for up and down spins which is unity for zero magnetization [14]. Otherwise, projection on the sites of cluster B is performed exactly and leads effectively to a trial wavefunction for the antiferromagnet on cluster B.

Projection on cluster B involves evaluating the expectation of a product of fermion operators in the non-interacting ground state. By Wick's theorem, this product can be reduced to products of single-particle correlation functions such as $\langle \psi \mid c_{i\sigma}^{\dagger}\, c_{j\sigma} \mid \psi \rangle$ or $\langle \psi \mid c_{i\sigma}^{\dagger}\, c_{j\ -\sigma}^{\dagger} \mid \psi \rangle$. Such correlation functions can be determined from the single-particle states and their occupation. The choice of points in cluster B is one which includes as many near neighbours of i and j as possible. This approximation tends to the exact result in the limit of infinite cluster size but practically we are limited to cluster sizes of about 15 sites. Projection on a cluster of 12 sites with complex fermion correlations takes about one hour on a Sun Sparc I workstation.

To assess the accuracy of this approximation technique, it was applied to the 1D Heisenberg spin chain. The results were compared with exact analytic Gutzwiller projection [15]. We list in tables 1 and 2 the values calculated for the spin–spin correlation functions of the projected one-dimensional Fermi sea at half filling. In table 1 we plot the nearest-neighbour correlation on a link as a function of distance

Table 1. Nearest-neighbour correlation $\langle S_n^z S_{n+1}^z \rangle$ in one dimension as a function of position from the centre ($n = 0$) of the cluster and cluster size.

Cluster size	$n = 0$	$n = 1$	$n = 2$	$n = 3$	$n = 4$	Cluster average
8	−0.13914	−0.15608	−0.13713	−0.16251	—	−0.15008
9	−0.14662	−0.14980	−0.14244	−0.15772	—	−0.14915
12	−0.14169	−0.15321	−0.14110	−0.15461	−0.13825	−0.14901
13	−0.14699	−0.14855	−0.14523	−0.15087	−0.14163	−0.14861

Table 2. *Averaged correlation $\langle S_0^z S_n^z \rangle$ as a function of separation n in one dimension* obtained from the 13-site cluster.

	$n = 1$	$n = 2$	$n = 3$	$n = 4$	$n = 5$	$n = 6$
Cluster method	−0.14861	0.05676	−0.04482	0.02994	−0.02627	0.02037
Exact [15]	−0.147373	0.056423	−0.044425	0.029686	−0.026005	0.020134

of the link from the centre of the cluster for different cluster sizes. Here clusters have been chosen to be sets of contiguous sites on the one-dimensional chain. In table 2 we tabulate longer distance correlation functions.

The effects of finite cluster size and the breaking of translational invariance are apparent. We neglect projection outside the cluster and the effect of that is greatest at the boundary of the cluster but extends far into the middle. For example for the 13-site cluster the nearest-neighbour correlation oscillates about an average value −0.1486 compared to the exact value of −0.1474. Finite cluster size leads to an inequivalence between certain sites which would be equivalent in the infinite system. This plagues any finite-cluster analysis including extrapolation of small-cluster diagonalization. If we wish to estimate a certain spin–spin correlation of the infinite system a simple but naive fix is to average over corresponding pairs in the cluster. The error in approximating the infinite system may then be assessed by examining cluster size dependence. We have checked this for 8–13-site clusters in one dimension. Notice in table 2 that longer range spin correlations (up to sixth-neighbour) given by the cluster technique are accurate to within one per cent. In two dimensions fermion correlation functions fall off with one higher power of distance but the fraction of sites at the surface of a small cluster is also larger. There is evidence from the square lattice that the cluster expansion in two dimensions is potentially quite accurate even for determining correlations out to the surface of the cluster [13]. This remains true when the cluster size is as small as four or even two sites. We have checked that the average values of spin–spin correlations are independent of cluster size up to and including the two largest clusters presented in this paper.

Spin correlation of a projected fermion wavefunction are usually evaluated using the variational Monte Carlo (VMC) technique [16]. VMC is computationally intensive compared to the cluster method. Finite-system fermion wavefunctions are used in VMC and these need to be continually re-evaluated—a process that is time consuming. Nevertheless the projection is carried out exactly ensuring accuracy (especially) in long-range spin–spin correlations. The cluster method has an advantage in being more transparent due to its analytical foundation. The density matrix of single-particle correlations is determined once for the infinite system at the beginning. Although it is weaker on the many-body aspects of projection, the technique enables the short-

range correlations to be calculated quickly. In this work, we assess the projection of many different fermion wavefunctions with various perturbations. Using the cluster technique it is easy to see how changes in the fermion wavefunction affect the spin–spin correlations. Thus we can obtain some understanding of why a particular large-n mean field saddle point is good or not.

3. The trial states

Let us begin by describing the fermion states we project and tabulating various short-range correlation functions for these many-fermion states. In all cases the fermion state will be described by the ground state of some fermion Hamiltonian. The simple hopping Hamiltonian

$$H = \sum_{\langle ij\rangle,\sigma} c^{\dagger}_{i\sigma} c_{j\sigma} + \text{HC}$$

(where $\langle ij\rangle$ means sum over nearest neighbours) on the Kagomé lattice has energy bands

$$\epsilon_k = -2 \qquad 1 \pm \sqrt{3 + 2(\cos k_1 + \cos k_2 + \cos k_3)} \tag{2}$$

where $k_3 = -(k_1 + k_2)$. The momentum components are defined by $k_i = \boldsymbol{k} \cdot \hat{\tau}_i$. Figure 1 shows the unit vectors τ_i. The bands do not have particle–hole symmetry. To make the no-flux pre-projection state we fill the states below a chemical potential $\mu \equiv -0.4715$ corresponding to half filling.

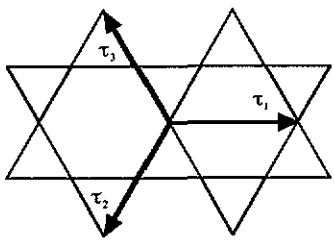

Figure 1. Unit vectors defined for the Kagomé lattice.

Another trial wavefunction is formed by using single-particle states in the presence of a staggered magnetic flux $\phi_0/4$ where $\phi_0 \equiv hc/e$ is the flux quantum. The gauge choice is shown in figure 2. An arrow on a link connecting site n to site m means that the terms in the Hamiltonian which hop electrons from site n to site m and m to n are multiplied by $+\mathrm{i}$ and $-\mathrm{i}$ respectively. Diagonalization leads to three energy bands which are the solutions to

$$\epsilon_k^3 - 2(3 + \cos k_1 + \sin k_2 + \sin k_3)\epsilon_k - 4(-\sin k_1 + \cos k_2 + \cos k_3) = 0. \tag{3}$$

The spectrum is particle–hole symmetric. For half filling there is a triangular Fermi surface at $\epsilon_k = 0$. The negative energy fermion states are filled before projection.

A third trial wavefunction corresponds to fermions hopping on a lattice with a uniform magnetic flux $\phi_0/4$. The gauge choice is given in figure 3. There are six energy bands which are well separated and are the solutions to

$$\epsilon_k^6 - 12\epsilon_k^4 + 2\epsilon_k^2(15 + \cos 2k_2 - 2\cos k_1 \cos k_2) - 16 = 0. \tag{4}$$

The lowest three are filled. In order to test robustness we also considered perturbations of this trial state which consisted of adding second-neighbour hopping of various magnitudes and phases.

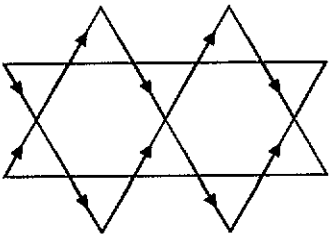

Figure 2. Gauge choice for the staggered flux Hamiltonian.

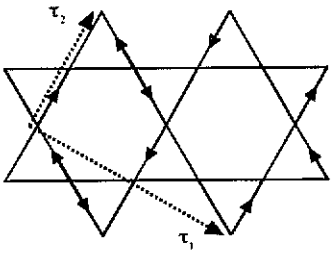

Figure 3. Gauge choice and unit vectors for the uniform flux Hamiltonian.

A second class of trial wavefunctions are the projected BCS wavefunctions. Affleck *et al* [17] exploited a local SU(2) gauge invariance to show that on a bipartite lattice a projected BCS state is identical to some projected non-BCS state. However, this cannot be done on a frustrated lattice and the projected BCS states are distinct from non-BCS ones. The simplest BCS state is the ground state of

$$H = \sum_{\langle ij \rangle} c_{i\uparrow}^\dagger c_{j\downarrow}^\dagger + \text{HC}$$

We considered BCS states with an amplitude modulation (spin–Peierls perturbation) or various arrangements of a non-trivial phase $ic_{i\uparrow}^\dagger c_{j\downarrow}^\dagger$ + HC. The latter was motivated by analogy to the '$s + id$' phase of Kotliar [11] The spin–Peierls perturbations were chosen to enhance the singlet pair amplitude along certain links in the dimer covering pattern shown in figure 4.

In table 3 we list the ground-state fermion correlations $|\langle c_n^\dagger c_0 \rangle|$ at half filling for each of the translationally invariant fermion states. In the non-BCS states the complex phases of $\langle c_n^\dagger c_0 \rangle$ depend on the choice of gauge but the magnitudes are

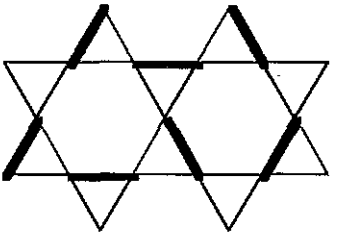

Figure 4. Dimer covering pattern used in making states with spin–Peierls order. The heavy lines represent bonds with enhanced spin singlet pairing amplitude.

translationally invariant and depend only on the flux. The notation of Zeng and Elser [6] is used to identify pairs of sites. For example $\langle 2\ \sqrt{3}\rangle$ refers to two points, 0 and n, which are second-nearest neighbours and separated by a distance of $\sqrt{3}$ lattice constants. Notice that the numbers for uniform flux are much more precise. That is because the fermion spectrum has a gap and so the Fermi level is clearly defined. In the case of BCS states the non-zero correlations are $\langle c^{\dagger}_{n\uparrow} c^{\dagger}_{0\downarrow}\rangle$. The BCS Hamiltonian happens to favour a mean occupancy such that $\langle c^{\dagger}_{0\sigma} c_{0\sigma}\rangle = 0.5$. There were minor computational problems for the BCS state with non-zero phases. They led to a breaking of translational invariance in the magnitude of pre-projection fermion correlations by a few per cent.

Table 3. Magnitude of the fermion correlation function on the Kagomé lattice $|\langle c^{\dagger}_{n} c_{0}\rangle|$ for various pairs of sites in various preprojection fermion wavefunctions. For the BCS case $\langle c^{\dagger}_{n\uparrow} c^{\dagger}_{0\downarrow}\rangle$ is tabulated. See the text for an explanation of the notation used to identify pairs of sites.

	$\langle 0\ 0\rangle$	$\langle 1\ 1\rangle$	$\langle 2\ 2\rangle$	$\langle 2\ \sqrt{3}\rangle$	$\langle 3\ 2\rangle$	$\langle 3\ \sqrt{7}\rangle$	$\langle 3\ 3\rangle$
No flux	0.5	0.2161	0.0773	0.0389	0.0105	0.0090	0.0220
Staggered	0.5	0.2169	0.0650	0.0	0.0296	0.0087	0.0579
Uniform	0.5	0.22478	0.0	0.08804	0.08702	0.01252	0.01042
BCS (no phase)	−0.0833	0.2204	−0.0235	−0.0151	−0.0544	−0.0107	−0.0405

4. Results

Table 4 shows spin–spin correlations between various pairs of sites. In the same table are listed the (21-site) cluster-averaged correlations of Zeng and Elser. The same notation as table 3 is used to identify pairs of sites. Results for 9- and 12-site clusters (shown in figure 5) are given in order to give an idea of the dependence of our results on cluster shape and size. In order to show finite size effects we have tabulated both the values of spin–spin correlations between symmetry inequivalent pairs as well as the cluster average. If there are two or more inequivalent pairs of sites for a given separation these correlations are listed starting from the innermost pairs. The projected BCS case was considered on at most a 9-site cluster because of computational limitations.

Table 4. Spin–spin correlation function $\langle S_0^z S_n^z \rangle$ for various pairs of sites in various projected fermion wavefunctions. Where there are inequivalent pairs of sites at a given separation the correlations are listed starting from the innermost pairs. See the text for an explanation of the notation used to identify pairs of sites.

	$\langle 1\ 1 \rangle$	$\langle 2\ 2 \rangle$	$\langle 2\ \sqrt{3} \rangle$	$\langle 3\ 2 \rangle$	$\langle 3\ \sqrt{7} \rangle$
No flux (9 sites)	−0.0687	−0.0012	0.0132	−0.0019	−0.0007
	−0.0687	—	—	—	—
	−0.0721	—	—	—	—
Average	−0.0696	−0.0012	0.0132	−0.0019	−0.0007
No flux (12 sites)	−0.0668	−0.0013	0.0129	−0.0036	−0.0001
	−0.0706	—	0.0135	—	—
Average	−0.0693	−0.0013	0.0132	−0.0036	−0.0001
Staggered (9 sites)	−0.0643	0.0010	0.009	−0.0029	0.0009
	−0.0660	—	—	—	—
	−0.0717	—	—	—	—
Average	−0.0670	0.0010	0.009	−0.0029	0.0009
Staggered (12 sites)	−0.0621	0.0009	0.009	−0.0034	0.0008
	−0.0682	—	0.010	—	—
Average	−0.0662	0.0009	0.0095	−0.0034	0.0008
Uniform (9 sites)	−0.0665	0.0103	−0.0043	−0.0120	0.0021
	−0.0674	—	—	—	—
	−0.0758	—	—	—	—
Average	−0.0693	0.0103	−0.0043	−0.0120	0.0021
Uniform (12 sites)	−0.0635	0.0103	−0.0036	−0.0090	0.0015
	−0.0708	—	−0.0050	—	—
Average	−0.0684	0.0103	−0.0043	−0.0090	0.0015
BCS (9 sites)	−0.0656	0.0055	0.0107	−0.0053	−0.0011
	−0.0764	—	—	—	—
	−0.0457	—	—	—	—
Average	−0.0660	0.0055	0.0107	−0.0053	−0.0011
Small cluster [6]	−0.07279	0.01369	0.00974	±0.0004	±0.017

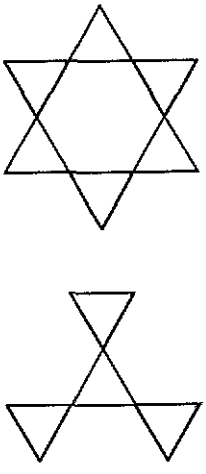

Figure 5. The 9- and 12-site clusters used in projection.

The error in estimating, say, the nearest-neighbour correlation of the infinite system by the cluster average is not nearly as large as the spread in numerical values of correlations between symmetry inequivalent pairs throughout the cluster. That was shown by the test on the one-dimensional chain. Moreover on comparing cluster averages for the 9- and 12-site clusters in table 4 we see very little difference up to second-neighbour correlations. The conclusions of this paper will be based on gross qualitative features of these correlations and so will not be sensitive to the small errors indicated by the 9- to 12-site cluster comparison.

All the trial wavefunctions have reasonably good energy so from that standpoint the ground state could have any of the symmetries represented by the trial wavefunctions. One could imagine adjusting the fermion wavefunctions a little bit to improve the energy. However, when other correlations are examined it is clear how these trial states differ qualitatively from the ground state.

The 'no flux' state differs mostly in the $\langle 2\ 2\rangle$ correlation where it is slightly antiferromagnetic. The small-cluster result shows a substantial ferromagnetic correlation. The 'staggered flux' state shows almost no correlation between $\langle 2\ 2\rangle$ pairs. Looking at the third column of table 3 we see that the lack of ferromagnetic correlations may be traced to a large exchange hole in the pre-projection fermion state. In the 'staggered flux' state there is also a bit too much antiferromagnetic correlation at $\langle 3\ 2\rangle$. The 'uniform flux' state has antiferromagnetic correlations between $\langle 2\ \sqrt{3}\rangle$ and $\langle 3\ 2\rangle$ which disagree with small cluster results. Again they can be traced to the corresponding fermion correlations.

Since we were able to trace deficiencies in spin–spin correlations to specific second-neighbour fermion correlations it was natural to try to alter these by including explicit second-neighbour hopping as a variational parameter. After an extensive search we were unable to find any combination of second-neighbour hopping which improved the energy.

The projected BCS wavefunction most resembles the ground state. However, it is still significantly deficient in the correlations $\langle 2\ 2\rangle$ and $\langle 3\ 2\rangle$. Upon perturbing this state by including phases we found that phases strongly increased the amount of ferromagnetic correlation in a link and so never helped the variational energy. Pairing magnitude perturbations of 10% and 20% were examined. These caused spin–Peierls like variations in near-neighbour $\langle S_0^z S_1^z\rangle$ of roughly 20% and 40% respectively. The former perturbation lowered the energy by about one per cent while the latter did not improve the energy noticeably. More significant however is the fact that the correlations $\langle 2\ 2\rangle$ and $\langle 3\ 2\rangle$ remained unchanged to within ± 0.001. Small errors may affect the comparison of relative variational energies but the order-one discrepancies in the above correlations were definitely not fixed by spin–Peierls order.

5. Discussion

One reason why translationally invariant projected fermion trial states may do poorly is that the exact ground state on some of the smaller clusters which may be formed in the Kagomé net are valence bond solids. The five-site 'hourglass' cluster is one of these. The ground state is sixfold degenerate and has the property that the spins at the bottom or top two sites of the hourglass are never parallel. Using this fact one can prove that the ground state cannot be formed from the projection of electrons in the lowest energy eigenstates of some uniform magnitude hopping Hamiltonian.

This feature that the 'hourglass' ground state lacks means that there is no simple generalization to the whole lattice. Rokhsar [18] has pointed out that on simple short closed loops the exact ground state is obtained by projecting fermions with the right amount of flux. In that case it is easy to generalize a set of flux rules to the whole lattice or understand why flux wavefunctions might work well. Obviously a slight complication such as the joining of one pair of next-nearest neighbours ruins this picture. Here it is worthwhile to note that the simple uniform flux prescription fails badly on the triangular lattice [19].

The original motivation for examining the projected fermion states was that they represented large-n saddle points. Optimizing a spin state by a large-n mean field approach is equivalent to assuming that the nearest-neighbour exchange hole is a monotonic function of the kinetic energy of the filled Fermi sea. It is also equivalent to assuming that the spin energy is proportional to the exchange hole. There are two problems that this approach encounters. Firstly, there is no general relation between kinetic energy and exchange. For certain cases—a square lattice with flux 0 or $\phi_0/2$ or on the 1D chain—the exchange hole is simply proportional to the square of the kinetic energy. Perhaps that is why flux states work well there. But there is no universal relation. Secondly, although the nearest-neighbour correlation hole is the dominant factor in determining the variational energy, the more distant neighbours can also affect the nearest neighbour spin–spin correlations resulting after Gutzwiller projection.

Let us consider what correlations might be missing. The valence bond solid perturbation considered did not improve on our projected BCS trial state very much. Of course one could impose spin–Peierls perturbations starting from other states. Also there are other dimer configurations to consider (Marston and Zeng proposed one with an 18-site unit cell—this was too large for us to handle). But we do not believe that correlations between certain second- and third-neighbour spins can ever be made more ferromagnetic by spin–Peierls order.

Another possibility for a missing correlation is insufficient short-range three-sublattice Néel order. This particular correlation is not accessable in the SU(n) large-n formalism. In a study of the simple flux wavefunction *ansatz* on the square lattice AFM [20], Néel order was found to be lacking. Because of the classical degeneracy mentioned in the introduction, there are different choices of sublattice arrangement on the Kagomé net. Based on our numerical results we are able to suggest that the sublattice arrangement shown in figure 6 is favoured by quantum fluctuations (represented by our projected fermion trial states). The opposite corners in every hexagon are in the same sublattice and every sublattice appears in every hexagon. The clusters for which the magnetization can be rotated without affecting the classical spin energy are linear chains. This choice would make $\langle 2\ 2\rangle$ and $\langle 3\ 2\rangle$ more ferromagnetic (by the roughly the same amount) while making $\langle 2\ \sqrt{3}\rangle$ more antiferromagnetic. It would seem to move these correlations of the no-flux and projected BCS state in the right direction as evidenced by the data in table 4. Projected fermion states with Néel order were not examined. The presence of three sublattices, each with separate magnetization direction, is difficult to deal with. The Néel order parameter involves spin-flip terms which essentially doubles the number of fermion single-particle correlation functions which need to be considered.

Finally we address a possible phase transition at finite temperature as suggested by Elser's interpretation [2] of the heat capacity data of Greywall and Busch. From table 4 one may see that a sudden decrease in the $\langle 2\ \sqrt{3}\rangle$ correlation might indicate a

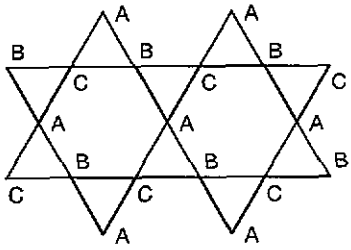

Figure 6. Proposed sublattice arrangement for local Néel order.

transition to a chiral spin liquid state as proposed by Marston and Zeng. Transitions to other states may also be detected by tracking the appropriate two-spin correlations. In this case of flux states the proper order parameter would be $S_1 \cdot S_2 \times S_3$ where 1,2,3 denote vertices of a triangle. We have not calculated the expectation of this three-spin operator.

6. Conclusion

The projected fermion wavefunctions we have examined have been shown to be qualitatively different from the ground state. That implies that the corresponding large-n saddle points are not associated with the correct ground state. We have argued that the missing correlations appear to be those of short-range Néel order rather than spin–Peierls order. Néel order cannot be implemented in SU(n) theories but can in principle be implemented in Sp(n) formalism, although the three sublattices and three magnetization axes complicates matters (just as it complicates the evaluation of the projected fermion wavefunction). One corollary of our claim is that the ground state does not have an excitation energy gap. The large-n saddle point states considered here are not candidates for the ground state but might be appropriate for higher temperature phases. To detect phase transitions to particular states we could track the behaviour of particular two-spin correlations. While such correlations are not strictly order parameters they are generally easier to measure than higher order spin–spin correlations.

Acknowledgments

This work was begun in Trieste, Italy at the ICTP 1990 workshop on strongly correlated electrons. TCH is supported by the Natural Sciences and Engineering Research Council of Canada and the Killam foundation. AJS is supported by the Science and Engineering Research Council of the United Kingdom, Smith Associates Limited and the Schiff Foundation. We wish to acknowledge conversations with P Chandra, J B Marston, I Ritchey and J M Wheatley.

References

[1] Greywall D S and Busch P A 1989 *Phys. Rev. Lett.* **62** 1868; 1990 *Phys. Rev. Lett.* **65** 2788
Greywall D S 1990 *Phys. Rev.* B **41** 1842

[2] Elser V 1989 *Phys. Rev. Lett.* **62** 2405
[3] Ramirez A P, Espinosa G P and Cooper A S 1990 *Phys. Rev. Lett.* **64** 2070
[4] Broholm C, Aeppli G, Espinosa G P, Cooper A S 1990 *Phys. Rev. Lett.* **65** 3173
[5] This point was made to us by P Chandra.
[6] Zeng C and Elser V 1990 *Phys. Rev.* B **42** 8436
[7] Marston J B and Zeng C 1991 *J. Appl. Phys.* **69** 5962
[8] Chandra P, Coleman P and Larkin A I 1990 *J. Phys.: Condens. Matter* **2** 7933
[9] Sachdev S and Read N 1991 *Int. J. Mod. Phys.* B. **5** 291
[10] Baskaran G, Zou Z and Anderson P W 1987 *Solid State Commun.* **63** 973
[11] Kotliar G 1988 *Phys. Rev.* B **37** 3664
[12] Zhang F C *et al* 1988 *Supercond. Sci. Tech.* **1** 36; 1990 *Phys. Rev. Lett.* **64** 974
[13] Hsu T C 1990 *Phys. Rev.* B **41** 11379
[14] Hsu T C, Marston J B and Affleck I 1991 *Phys. Rev.* B
[15] Gebhard F and Vollhardt D 1987 *Phys. Rev. Lett.* **59** 1472
[16] Ceperley D, Chester G V and Kalos M H 1977 *Phys. Rev.* B **16** 3081
[17] Affleck I, Zou Z, Hsu T and Anderson P W 1988 *Phys. Rev.* B **38**
[18] Rokhsar D S 1990 *Phys. Rev. Lett.* **65** 1506; 1990 private communication
[19] Anderson P W, Shastry B S and Hristopoulos D 1989 *Phys. Rev.* B **40** 8939
[20] Lee T-K and Feng S-P 1988 *Phys. Rev.* B **38** 11809